Comparative analysis of Archaeal lipid-linked oligosaccharides that serve as oligosaccharide donors for Asn-glycosylation

田口, 裕也

https://doi.org/10.15017/1806840

出版情報：九州大学, 2016, 博士（システム生命科学）, 課程博士
バージョン：

Comparative analysis of Archaeal lipid -linked oligosaccharides that serve as oligosaccharide donors for Asn-glycosylation

（古細菌のＮ型糖鎖供与体（脂質結合型糖鎖）の比較分析）

田口 裕也

ABBREVIATIONS

*Af*AglB	*Archaeoglobus fulgidus* AglB
Agl	archaeal glycosylation
DDM	n-dodecyl β-D-maltoside
dHex	deoxyhexose
Dol-P	dolichol-monophosphate
Dol-PP	dolichol-diphosphate
ESI-MS	electrospray ionization tandem mass spectrometry
Hex	hexose
HexA	hexuronate
LC	liquid chromatography
LLO	lipid-linked oligosaccharide
NAc	N-acetyl
NPLC	normal phase LC
OG	β-octylglucoside
OST	oligosaccharyltransferase
*Pc*AglB	*Pyrobaculum calidifontis* AglB
*Pf*AglB	*Pyrococcus furiosus* AglB
QuiS	sulfoquinovose
RPLC	reverse-phase LC
TIC	total ion chromatogram
*Ss*AglB	S*ulfolobus solfataricus* AglB
TAMRA	carboxytetramethylrhodamine
TM	transmembrane;
XIC	extracted ion chromatogram.

Contents

1. ABSTRACT

The glycosylation of asparagine residues is the predominant protein modification in all three domains of life. An oligosaccharide chain is preassembled on a lipid-phospho carrier, and transferred onto asparagine residues by the action of a membrane-bound enzyme, oligosaccharyltransferase. The oligosaccharide donor for the oligosaccharyl transfer reaction is dolichol-diphosphate-oligosaccharide (Dol-PP-OS) in Eukaryota, and polyprenol-diphosphate-oligosaccharide (Pren-PP-OS) in Eubacteria. The donor in some archaeal species was reportedly dolichol-monophosphate-oligosaccharide (Dol-P-OS). Thus, the difference in the number of phosphate groups aroused interest in whether the use of the Dol-P type donors is widespread in the domain Archaea. Currently, all of the archaeal species with identified oligosaccharide donors have belonged to the phylum Euryarchaeota. Here, we analyzed the donor structures of two species belonging to the phylum Crenarchaeota, *Pyrobaculum calidifontis* and *Sulfolobus solfataricus*, in addition to two species from the Euryarchaeota, *Pyrococcus furiosus* and *Archaeoglobus fulgidus*. The ESI-MS analyses confirmed that the two euryarchaeal oligosaccharide donors were the Dol-P type, and newly revealed that the two crenarchaeal oligosaccharide donors were the Dol-PP type. This novel finding is consistent with the hypothesis that the ancestor of Eukaryota is rooted within the TACK (Thaum-,Aig-, Cren-, and Korarchaeota) superphylum, which includes Crenarchaea. Our comprehensive study also revealed that one archaeal species could contain two distinct oligosaccharide donors for the oligosaccharyltransfer reaction. The *A. fulgidus* cells contained two oligosaccharide donors bearing oligosaccharide moieties with different backbone structures, and the *S. solfataricuscells* contained two oligosaccharide donors bearing stereochemically-different dolichol chains.

2. INTRODUCTION

The glycosylation of asparagine residues is the predominant protein modification throughout all three domains of life (1-3). The oligosaccharides attached to asparagine residues in glycoproteins (N-glycan) affect various properties of the proteins, including folding, conformation, solubility, and antigenicity. Carbohydrate-binding proteins, such as lectins, recognize the N-glycans. Within the lumen of the endoplasmic reticulum in eukaryotic cells, the N-glycan functions as a quality-control tag in the ER-associated degradation (ERAD) (4). The N-glycosylation occurs in the consensus motif (referred to as the sequon) represented by Asn-X-Ser/Thr, where X can be any residue except Pro. The formation of the N-glycosidic bond, between the monosaccharide residue at the reducing end of an oligosaccharide and the side-chain amide group of the asparagine residues in proteins, is catalyzed by a membrane-bound enzyme, oligosaccharyltransferase (OST) (3). The eukaryotic OST enzyme is a multi-subunit protein complex. Among the eight different membrane subunit proteins, the catalytic subunit is a polypeptide chain called STT3. In contrast, the lower eukaryotic protozoan OST is a single subunit enzyme consisting of only STT3. The archaeal and eubacterial OSTs are also single subunit enzymes, consisting of AglB and PglB, respectively. Although the catalytic subunits are referred to differently among the three domains of life, they have a common ancestor, and share several conserved short sequence motifs (5). The crystal structures of the AglB and PglB proteins revealed common protein architectures, consisting of an N-terminal transmembrane (TM) region containing 13 TM helices, and a C-terminal soluble, globular domain (6,7). The C-terminal globular domain possesses a binding pocket that recognizes the hydroxy amino-acid residue in the N-glycosylation sequon. When the Ser/Thr-binding pocket interacts with the sequon, two conserved acidic residues in the N-terminal TM region transiently form a catalytic structure with a bivalent metal ion, to activate the acceptor asparagine side chain in the sequon. After the transfer reaction, glycosidase- and glycotransferase-mediated processing reactions trim, elongate, and branch the nascent N-glycans, in the ER and Golgi of eukaryotic cells (8). Although it was long thought that no post-transfer N-glycan processing occurs in Archaea, the first instance was recently discovered: a terminal mannose residue was added to the

four-residue N-glycan on a protein on the exterior side of the cell membrane in the halophilic archaeon, *Haloferax volcanii* (9). No post-transfer N-glycan processing has been reported in eubacterial cells.

The oligosaccharide donor for the OST enzyme is a lipid-linked oligosaccharide (LLO), in which an oligosaccharide chain is preassembled on a lipid-phospho carrier. In Eukaryotes from yeast to human, 14 monosaccharide residues are assembled onto the lipid-phospho carrier by the sequential actions of many glycotransferases (2). In lower Eukaryotes, such as Protozoa and Fungi, trimmed versions of the 14-residue glycan are used (10). Archaea and Eubacteria use their own sets of glycotransferases to assemble distinct oligosaccharides on their unique lipid-phospho carriers (2,11). Consequently, wide diversity is observed in the archaeal and eubacterial N-glycan structures, in terms of the sizes, compositions, branching patterns, and chemical modifications of the constituent monosaccharides (1,12).

The eukaryotic and eubacterial N-glycosylation systems have been extensively studied, both genetically and biochemically, primarily in the yeast, *Saccharomyces cerevisiae*, and the foodborne pathogen, *Campylobacter jejuni*, as model organisms (2). Detailed knowledge of the archaeal N-glycosylation has also been accumulated through intensive studies of a few model organisms, including *H. volcanii*, *Methanococcus voltae*, *Methanococcus maripaludis*, and *Sulfolobus acidocaldarius* (13,14). However, due to the huge diversity in the N-glycosylation system in Archaea, extensive studies are still required to clarify the generality of the knowledge obtained from these model species. The complicated pathway of LLO biosynthesis in *H. volcanii* has been studied by Eichler's group for the past decade. Taking advantage of the established gene knockout method, the functions of the Agl (archaeal glycosylation) proteins, including AglB, were investigated in detail (15,16). In parallel, they performed the NPLC-ESI-MS/MS (normal-phase liquid chromatography-electrospray ionization tandem mass spectrometry) analysis of total lipid extracts from cultured cells, to elucidate the chemical structures of the LLOs. In addition to *H. volcanii*, they analyzed the LLOs from other haloarchaea, including *Halobacterium salinarum*, *Haloferax mediterranei*, and *Haloarcula marismortui* (17). They also extended their MS analysis to the LLOs from

non-haloarchaea, including the thermoacidophilic archaeon, *S. acidocaldarius* (18), and the hyperthermophilic archaeon, *Pyrococcus furiosus* (19). In all of the cases, an oligosaccharide-charged dolichol-monophosphate (Dol-P) was identified. Dolichol is a polyprenol (i.e., a long-chain isoprenoid alcohol) that contains a saturated isoprene unit at the α-position. Isoprenoids are comprised of various numbers of the 5-carbonisoprene units, $(-CH_2-CH=C(CH_3)-CH_2)_n$. The dolichol chain of the eukaryotic LLOs is long, comprising 14 to 22 isoprene units (i.e.,C70-C110), whereas that of the archaeal LLOs is shorter (C55-C60) (20). The special quality of the archaeal LLOs is that the dolichol moiety is highly saturated: The double bonds in the isoprene units are saturated at various degrees (1-5 saturated isoprene units) in the proximity of the ω-position (19). Finally, the lipid part of the eubacterial LLOs for PglB is polyprenol (C45-C60), which has an unsaturated isoprene unit at the α-position (20).

In *H. marismortui*, the Dol-P-charged oligosaccharide was the same as the N-glycan attached to the glycoproteins (21). In other cases, shorter oligosaccharides were found in the Dol-P type LLOs. There are multiple explanations for the truncated oligosaccharides. In *H. volcanii*, the difference is due to the post-transfer modification of the N-glycan, as mentioned above (9). Another possibility is that the LLOs with shorter oligosaccharides are precursors in the LLO biosynthesis or breakdown products generated during the lipid preparation. To demonstrate that the Dol-P type LLO was actually the oligosaccharide donor for the N-glycosylation in *H. volcanii*, the changes in the oligosaccharide structures caused by the deletions of the agl genes were monitored on the Dol-P carrier and the S-layer glycoprotein (9,15,16). Imperiali's group provided direct biochemical evidence that the Dol-P-disaccharide indeed served as an oligosaccharide donor for the AglB from the methanogenic archaeon, *Methanococcus voltae* (22). These findings were surprising because the eukaryotic and eubacterial oligosaccharide donors contain two phosphate groups: oligosaccharide-charged dolichol-diphosphate (Dol-PP) and polyprenol-diphosphate (Pren-PP), respectively (20).

Exceptionally, in the total lipid extract from *H. salinarum*, a tetrasaccharide-charged Dol-PP was detected in addition to the Dol-P type LLO (17). The tetrasaccharide chain was similar,

but not identical to the N-glycan attached to the Asn-2 position of the *H. salinarum* S-layer glycoprotein reported previously (23). Thus, it is possible that both the Dol-PP type LLO and Dol-P LLO are oligosaccharide donors in *H. salinarum*. In summary, the oligosaccharide donors of the AglB enzymes in several archaeal species are the Dol-P type LLOs, but further studies are needed to clarify their general use within the domain Archaea. In this study, we selected four archaeal species, *Pyrococcus furiosus* and *Archaeoglobus fulgidus* from the phylum Euryarchaeota, and *Pyrobaculum calidifontis* and *Sulfolobus solfataricus* from the phylum Crenarchaeota. Euryarchaeota and Crenarchaeota are two well-studied phyla of the domain Archaea. The ESI-MS/MS analyses revealed that the purified LLOs of the two euryarchaeal species were Dol-P derivatives, whereas those of the two crenarchaeal species were Dol-PP derivatives. Their oligosaccharide donor activities were confirmed by oligosaccharyl transfer assays. Considering all of the present and previously reported data together, we concluded that the phylogenetic distributions of the two lipid-phospho carriers, Dol-P and Dol-PP, for the AglB enzymes closely match the archaeal phyla.

3. EXPERIMENTAL PROCEDURES

Cell cultures

Pyrococcus furiosus cells were a gift from Dr. Yoshizumi Ishino (Kyushu University). *Archaeoglobus fulgidus* strain NBRC100126 and *Sulfolobus solfataricus* strain NBRC15331 were obtained from the Biological Resource Center, the National Institute of Technology and Evaluation (NITE, Chiba, Japan). *Pyrobaculum calidifontis* strain JCM 11548 was obtained from Japan Collection of Microorganisms (JCM), the Microbe Division of RIKEN BioResource Center (BRC, Tsukuba, Japan). The growth medium for the *P. furiosus* culture consisted of 5.0 g yeast extract, 10 g starch, 10.8 g $MgCl_2 \cdot 6H_2O$, 24 g NaCl, and 4.0 g Na_2SO_4 per liter tap water. The growth medium for the *A. fulgidus* culture was the same as that used for the non-labeled culture in the previous study (24). The growth medium for the *P .calidifontis* culture consisted of 1.0 g yeast extract,10 g tryptone, and 3.0 g $Na_2S_2O_3 \cdot 5H_2O$ per liter tap water. The growth medium for the *S. solfataricus* culture consisted of 1.0 g yeast extract, 0.28 g KH_2PO_4, 0.25 g $MgSO_4 \cdot 7H_2O$, 80 mg $CaCl_2 \cdot 2H_2O$, 1.3 g $(NH_4)_2SO_4$, 14 mg $FeCl_2 \cdot 4H_2O$, 0.3 g $Na_2SiO_3 \cdot 9H_2O$, and 30 mg $Na_2MoO_4 \cdot 2H_2O$ per liter tap water, adjusted to pH 3.0 with H_2SO_4. The culture conditions were anaerobic, 98 °C, 18 h for *P. furiosus*; anaerobic, 80 °C, 3 days for *A. fulgidus*; aerobic, 90 °C, 2 days for *P. calidifontis*; and aerobic, 70 °C, 3 days for *S. solfataricus*. The typical cell yields were 1.6 g, 0.2 g, 0.3 g, and 0.6g wet cells from 1-liter culture medium of *P. furiosus*, *A. fulgidus*, *P. calidifontis*, and S. *solfataricus*, respectively. The *P. furiosus*, *P. calidifontis* and *S. solfataricus* cells were stored as glycerol stocks (50 % v/v) at -80 °C. The *A. fulgidus* cells were stored in a sealed glass vessel at room temperature, and subcultured every month.

Preparation of the membrane fractions from cultured cells

The cells were collected by centrifugation and disrupted in hypoosmotic buffer, consisting of 20 mM glycine-HCl, pH 2.8, for *S. solfataricus*, or 20 mM Tris-HCl, pH 7.5, and 2mM $MgCl_2$ for the other archaeal species. The cell disruption solutions were supplemented with benzonase (Novagen) and complete protein inhibitor cocktail, EDTA-free (Roche), according to the manufacturers' instructions. After the hypotonic treatment, the cell suspension was centrifuged at 8,500 g for 15 min, and the supernatant was discarded. The pellet was suspended in the buffer, and homogenized with a probe sonicator. After centrifugation for debris removal, the supernatant was ultracentrifuged at100,000 g for 2 h, to collect the

membrane fractions. The membrane pellets were stored at -80 °C until use.

Extraction of the LLOs from the membrane pellets

The membrane pellets were suspended in 20 mM glycine-HCl, pH 2.8, containing 0.1 M NaCl in the case of *S. solfataricus*, or in 20 mM Tris-HCl, pH 7.5, containing 0.1 M NaCl in the other cases. Aliquots were transferred into glass round-bottom centrifuge tubes. The *P. furiosus*, *P. calidifontis*, and *S. solfataricus* LLOs were extracted with a chloroform/methanol/water mixture, as described (25). The extraction method was originally used for yeast LLO extraction (26). The *A. fulgidus* LLO was prepared using a slightly different method, reported for the *H. volcanii* LLO extraction (9). This method is suitable for the extraction of more hydrophobic LLOs. The crude LLOs were dried in a SpeedVac concentrator (Thermo Savant), redissolved in a small volume of $CHCl_3$: CH_3OH : H_2O = 10 : 10 : 3 (v:v:v), and stored in glass containers at -20 °C.

Purification of LLOs by anion-exchange chromatography

LLOs were purified by anion-exchange chromatography with a HiTrap DEAE FF column (GE Healthcare), as reported previously (27). The crude LLO sample was applied to the column, which was equilibrated with $CHCl_3$: CH_3OH : H_2O = 10 : 10 : 3 (v:v:v) containing 3 mM acetic acid. Thirty minutes after the sample loading, the column was washed with the equilibrium solvent, and then the absorbed materials were eluted with $CHCl_3$: CH_3OH : H_2O = 10 : 10 : 3 (v:v:v), containing 0.3 M ammonium acetate. To adjust the chloroform/methanol/water composition, 0.43 ml of $CHCl_3$ and 0.12 ml of H_2O were added per 1 ml of the eluted solution. The mixture was vortexed vigorously, and then centrifuged. The lower organic phase was recovered, dried in a SpeedVac concentrator, and redissolved in a small volume of $CHCl_3$: CH_3OH : H_2O = 10 : 10 : 3 (v:v:v).

Purification of the LLOs by normal-phase HPLC and analysis by mass spectrometry

The LLOs were further separated on a SUPELCO column (4.6 mm Å~ 25 cm, 581513-u, Sigma-Aldrich), in essentially the same manner as that described for the analysis of *H. volcanii* LLO and Dol-P (9). Solvent A was $CHCl_3$: CH_3OH : NH_4OH = 800 : 195 : 5 (v:v:v), and solvent B was $CHCl_3$: CH_3OH : H_2O : NH_4OH = 450 : 450 : 95 : 5 (v:v:v:v). A linear gradient of solvent B was applied from 0 % to 100 %, at rates of 2 %/ml for the LLO analysis

and 4 %/ml for the Dol-P analysis. The flow rate was 1 ml/min. In the case of the *S. solfataricus* LLO, the initial percentage of solvent B was set to 30 %, and the flow rate was decreased to 0.5 ml/min, to avoid column clogging. A post-column splitter was used to deliver 10 - 20 % of the LC flow to the ESI source of a QSTAR Elite mass spectrometer (ABSciex), and the rest of the flow was fractionated for the enzymatic assay. The mass spectrometer settings in the negative ion mode were as follows: ion spray voltage, 4,500 V; curtain gas, 50 psi; ion source gas 1, 50 psi; ion source gas 2, 30 psi; temperature, 400 °C; declustering potential, 80 V; focusing potential, 250 V. Nitrogen gas was used as the collision gas.

Oligosaccharyl transfer assay

The recombinant AglB enzymes of the long paralog of *P. furiosus* (*Pf*AglB-L) and the long paralog and one of the two short paralogs of *A. fulgidus Af*AglB-L and *Af*AglB-S1) were expressed in *E.coli*, and purified to homogeneity in the presence of 1 % (w/v) n-dodecyl β-D-maltoside (DDM) (7,28,29). As alternatives to the recombinant AglB enzymes of *P. calidifontis* (*Pc*AglB) and *S. solfataricus* (*Ss*AglB), the LLO-depleted membrane fractions that contained the endogenous AglB proteins were prepared for the oligosaccharyl transfer assay. To obtain the *P. calidifontis* LLO-depleted membrane fractions, the membrane pellet was suspended in 20 mM Tris-HCl, pH 7.5, containing 0.5 M NaCl, 1 % β-octylglucoside (OG), and protein inhibitor cocktail, EDTA-free. The suspension was ultracentrifuged at 154,000 g for 1 h, to remove insoluble materials. An acceptor peptide, Ac-AAYNVTKRK(TAMRA)-OH (NVT peptide), in which TAMRA is a fluorescent dye attached to the side-chain amino group of the C-terminal Lys residue, was added at a final concentration of 2.5 μM to the OG-solubilized membrane fractions containing *Pc*AglB and LLO, to start the enzymatic reaction. The reaction solution was incubated at 80 °C for 4 h, to consume the endogenous LLO completely. The produced glycopeptide and the unreacted peptide substrate were removed by repeated ultrafiltration and dilution. The ultrafiltration was performed with an Amicon Ultra-4 centrifugal filter unit (30-kDa cutoff, Merck Millipore). The LLO-depleted membrane fractions were stored at 4 °C until use.

To obtain the *S. solfataricus* LLO-depleted membrane fractions, a slightly different method was used. The membrane pellet was suspended in 20 mM sodium acetate buffer, pH 4.6, containing 10 mM $MnCl_2$. The addition of the acceptor NVT peptide, at a final concentration

of 3.4 μM, started the reaction. The solution was incubated at 50 °C for 2 h, and then ultracentrifuged at 154,000 g for 1 h. The glycopeptide product and the unreacted peptide substrate remained in the supernatant, while *Ss*AglB was in the pellet. The pellet was resuspended in 20 mM Tris-HCl, pH 7.5, containing 0.5 M NaCl, 1 % OG, and protein inhibitor cocktail, EDTA-free. The OG in the buffer solubilized the *Ss*AglB. Insoluble materials were removed by ultracentrifugation for 1 h, and then the supernatant was recovered as the LLO-depleted membrane fraction containing *Ss*AglB. The LLO-depleted membrane fraction was stored at 4 °C until use.

The oligosaccharyl transfer activity was measured by the PAGE method (30). The NVT peptide was added at a final concentration of 2.5 μM. The reaction mixtures were incubated at 65 °C for 1 h for the assays using the recombinant *Pf*AglB-L, *Af*AglB-L, and *Af*AglB-S1; at 80 °C for 2 h for the assay using the LLO-depleted membrane fractions from *P. calidifontis*; and at 50 °C for 2 h for the assay using the LLO-depleted membrane fractions from *S. solfataricus*.

Analysis of lipid-phosphate products by normal-phase HPLC and mass spectrometry

To analyze the lipid-phosphate products of *Af*AglB-L, the NPLC fractions containing *A. fulgidus* LLOs (LLO-L and LLO-S) were combined and dried. The recombinant *Af*AglB-L, solubilized in 1 % DDM, and the NVT peptide (final concentration of 36 μM) were added to the dried LLO. Note that the final peptide concentration was about 10 times higher than usual, because the purified LLO was used. The reaction solution was incubated at 65 °C for 1 h. To analyze the lipid-phosphate product of the oligosaccharyl transfer reaction of *P. calidifontis*, the DDM-solubilized membrane fractions were mixed with the NVT peptide at a final concentration of 2.5 μM, and incubated at 80 °C for 2 h. To analyze the lipid-phosphate product of the oligosaccharyl transfer reaction of *S. solfataricus*, the OG-solubilized membrane fractions (50 mM sodium acetate, pH 4.6, 1 mM DTT, 1 % OG) were mixed with the NVT peptide at a final concentration of 2.5 μM, and incubated at 50 °C for 2 h. After 50-fold dilution with Solvent A, the reaction mixture was centrifuged at 16,000 g for 10 min, and filtered through Millex-GV syringe filter unit, 0.22 μm (Millipore). The resultant reaction solutions were directly injected into the normal-phase HPLC column, to analyze the MS structures of the lipid-phosphate products.

***MS analysis of the glycopeptide produced in the* P. calidifontis *membrane fraction*s**

The glycopeptide was prepared and analyzed according to the method used for *Pf*AglB-L (31). Briefly, the Triton X-100-solubilized membrane fractions contained both *Pc*AglB and LLOs, and the addition of the acceptor NVT peptide started the oligosaccharyl transfer reaction. After an incubation of the reaction solution at 80 °C for 1 h, the glycopeptide product was separated on a COSMOSIL 5C18-AR-II reverse-phase column (Nacalai Tesque, Kyoto, Japan), run in 0.1 % trifluoroacetic acid and acetonitrile. The glycopeptides were eluted by a linear gradient of acetonitrile, collected, and dried in a SpeedVac concentrator. The dried glycopeptide sample was dissolved in 0.1 % formic acid and 50 % methanol. The direct-infusion ESI-MS analysis was performed on the QSTAR Elite mass spectrometer in the positive ion mode.

Estimation of the composition of LLO species with various degrees of isoprene saturation

The isotopic distribution was calculated using the ChemCalc server, at http://www.chemcalc.org/ (32). After entering a chemical formula (e.g., C104H173O38N2P1 for *P. furiosus* LLO-L, S7:P1:C60:σ2), the simulated *m/z* - intensity data were returned in the XY data window. The FWHM (Peak Full Width at Half-Maximum) value was set to 0.1. The *m/z* - intensity data were transferred to Excel. In the Excel file, the intensity data of an LLO species with a certain saturation number (σ=2 in the example) were copied and pasted with an appropriate shift by *m/z* 2*1.01 (cf.$_1$H = 1.007825), to account for the difference in the degree of saturation. The intensity data for each *m/z* value were summed with specified weighting factors. The composition of LLO species with different degrees of saturation was estimated by manual adjustment of the weighting factors.

4. RESULTS

LLO quantification using LLO-depleted membrane fractions

For LLO quantification, an AglB preparation without LLO is required. Recombinant AglB proteins produced in a heterologous host, such as Escherichia coli, are suitable, but not always available. In spite of our attempts, the expression of the recombinant AglB proteins, from two species of Crenarchaeota, in *E. coli* cells was unsuccessful. The proteins were expressed at a trace level, but no enzymatic activity was detected. Alternatively, we prepared membrane fractions from the cultured archaeal cells. To remove the endogenous LLOs from the membrane fractions, an excess amount of an acceptor peptide was added. After the completion of the oligosaccharyl transfer reaction, the glycopeptide products, as well as the unreacted peptide substrates, were removed by repeated ultrafiltration and dilution steps.

ESI-MS/MS analysis of the glycopeptides produced in the membrane fractions of P. calidifontis

For the MS analyses of LLOs, the mass of the oligosaccharide part is required. The N-glycan structures of *P. furiosus* and *A. fulgidus* were determined by NMR spectroscopy (24,31). These structures were derived from the glycopeptides produced by in vitro enzymatic reactions, using the recombinant *P. furiosus* AglB-L and *A. fulgidus* AglB-L proteins. Here, the suffix L denotes the longest paralogous protein among the multiple AglB proteins. The oligosaccharide structure attached to the glycopeptide produced by the in vitro enzymatic reaction, using the recombinant *A. fulgidus* AglB-S1 (one of the two short paralogs), was estimated by MS spectrometry (29). The N-glycan structure of *S. solfataricus* glycoproteins was also estimated by MS spectrometry (33). In this case, the glycopeptides generated by tryptic/chymotryptic digests of the glycoproteins were used for the MS analysis. Finally, there was no information available about the structure of the N-glycan of *P. calidifontis*. Here, we used the in vitro method to prepare the glycopeptide, and determined its MS structure. The peaks in the reverse-phase (RP) LC chromatography were collected, and analyzed by the direct-infusion ESI-MS procedure in the positive ion mode. The triply-charged precursor ion was selected and subjected to the MS/MS analysis (Fig. 1). The N-glycan of *P. calidifontis*

consists of 10 monosaccharide residues, with the structureHex$_8$-HexA(NAc)$_2$-Hex(NAc)$_2$-Asn.

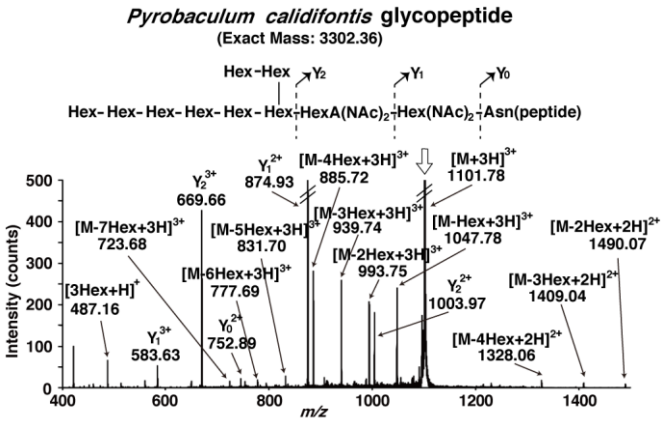

FIGURE 1. **ESI-MS/MS analysis of the glycopeptide produced in the *P. calidifontis* membrane fractions**. The Triton-X100 solubilized membrane fractions of the *P. calidifontis* cells were incubated with an acceptor peptide, Ac-AAYNVTKRK(TAMRA)-OH. The purified glycopeptide product was analyzed by direct-infusion ESI-MS/MS, in the positive ion mode. The triply-charged monoisotopic precursor ion is marked by the vertical arrow. The inset shows the predicted chemical structure of the glycopeptide, and the MS/MS fragmentation scheme. The branching structure of the N-glycan was determined by NMR analysis (unpublished data). The expected *m/z* values were observed within 0.02 of the theoretical mass values for triply-charged fragment ions.

NPLC-ESI-MS analyses of the total lipid extracts from the four Archaea

The membrane fractions of the four archaeal species were prepared from the cultured cells, by sonication and ultracentrifugation. The two-phase partitioning method with the chloroform/methanol/water solvent system was used to extract total lipids from the membrane fractions. The extracted crude lipids were further purified by anion-exchange chromatography. The absorbed materials were eluted with ammonium acetate, concentrated by two-phase partitioning, and then subjected to NPLC connected to a mass spectrometer, operated in the negative ion mode. The total ion chromatograms (TIC, ion chromatogram created by taking the summed intensities of all ions) of the NPLC-ESI-MS analyses are shown in Fig. 2. Simultaneously, the elution flow was split and fractioned. An aliquot of each fraction was assayed for the oligosaccharyl transfer activity. The purified recombinant enzymes or the LLO-depleted membrane fractions were added to the reaction solution. After incubation with a fluorescently labeled acceptor peptide, the formation of glycopeptide

products was monitored by the fluorescent imaging of the SDS-PAGE gels. The elution times of the fractions that produced the glycopeptides were closely matched with those of the TIC peaks. The coincidence indicated the high purity of the LLOs in the fractions from the NPLC column.

Figure 2 also shows the time-of-flight mass spectra (TOF-MS), which are the averaged mass scans acquired during the time periods indicated by the horizontal thick bars in the TIC charts. The constant *m/z* differences between the prominent peaks in the TOF-MS spectra suggested the existence of isoprene units (C_5H_8 = 68.06 amu). Considering the mass values after the subtraction of the oligosaccharide mass, we deduced the structures of the lipid-phospho carriers. In the analysis of the *P. furiosus* LLO (Fig. 2A), the $[M-2H]^{2-}$ ion peaks in the TOF-MS spectrum were a series of heptasaccharide-charged Dol-Ps containing C55, C60, and C65 dolichols. In the analysis of the *A. fulgidus* LLO (Fig. 2B), there were two TIC peaks corresponding to the LLOs bearing different seven-residue N-glycan structures, labeled as S7-L and S7-S, for which the $[M-2H]^{2-}$ ion peaks in the respective TOF-MS spectra were a series of mono-sulfated heptasaccharide-charged Dol-Ps containing C55 and C60 dolichols. In the analysis of the *P. calidifontis* LLO (Fig. 2C), the $[M-3H]^{3-}$ ion peaks were a series of decasaccharide-charged Dol-PPs containing C50 and C55 dolichols. Finally, in the analysis of the *S. solfataricus* LLO (Fig. 2D), there were two oligosaccharyl-transfer active peaks in the TIC chart, labeled as S6-A and S6-B. The $[M-3H]^{3-}$ ions in the respective TOF-MS spectra were hexasaccharide-charged C45 and C30 Dol-PPs.

The expansions of the TOF-MS peaks showed a deviation from the intensity distribution expected from the natural abundance of isotopes (Fig. 3, *left column*). The simulated MS spectra were calculated by assuming the saturation of the double bonds in some isoprene units (Fig. 3, *right column*). The molar ratios of the LLO species with different degrees of saturation were estimated by the manual adjustment of the weighting factors. The R^2 values of the peak intensity correlations between the raw and simulated mass spectra were sufficiently close to 1. As an exception, the correlation for the *P. calidifontis* LLO with a C50 dolichol moiety was found to be 0.905 (Fig. 3C). We repeated the MS simulation of other LLO species containing different numbers of isoprene units in the dolichol chain. Similar

compositions of the degree of saturation were obtained. In particular, the R^2 for the *P. calidifontis* LLO with a C55 dolichol moiety was as good as 0.993 (data not shown). Thus, we concluded that the mass distributions were attributed to the mixed state of the various degree of the double-bond saturation. All of the archaeal LLOs examined so far were highly saturated, with up to six isoprene units (19). The most extreme case was the *S. solfataricus*

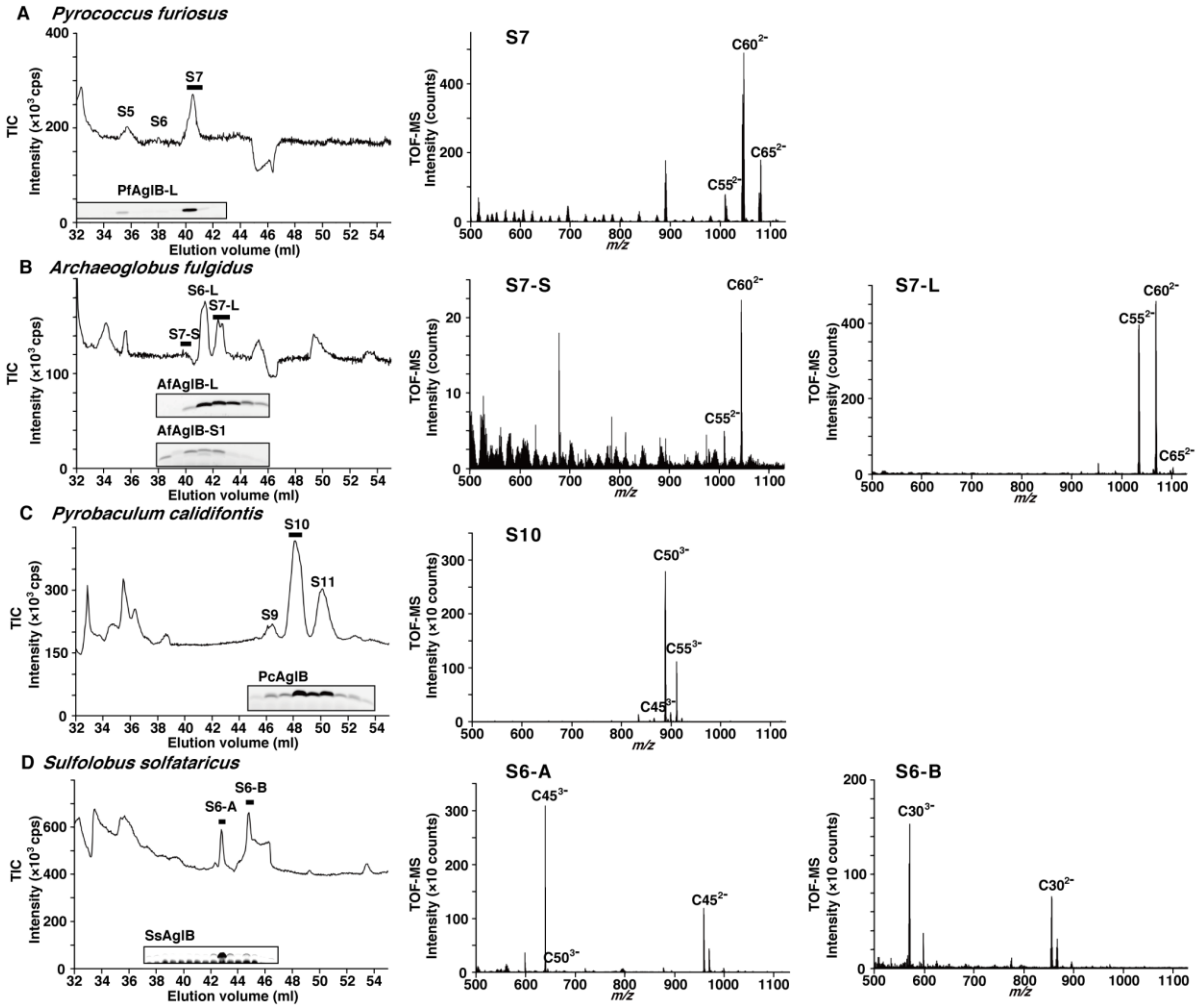

FIGURE 2. **Normal-phase LC-ESI-MS analyses of LLOs from four archaeal species.** The total lipid extracts of (*A*) *P. furiosus*, (*B*) *A. fulgidus*, (*C*) *P. calidifontis*, and (*D*) *S. solfataricus* were analyzed. The total ion chromatograms (TIC) of the ESI-MS analyses, and the TOF-MS spectra averaged from the mass scans acquired during the time period indicated by the horizontal thick bars in the TICs are shown. The symbol S in the TICs denotes the number of monosaccharide residues. The fluorescence images of the SDS-PAGE gels in the TICs are the results of the oligosaccharyl transfer assay. The bands in the gel images are the glycopeptides produced, and their intensities are proportional to the amounts of LLO in the NPLC fractions. Note that a contrast-enhanced fluorescence image of the SDS-PAGE gel is provided in Fig. 2D to shown the faint glycopeptide band corresponding to the S6-B peak.

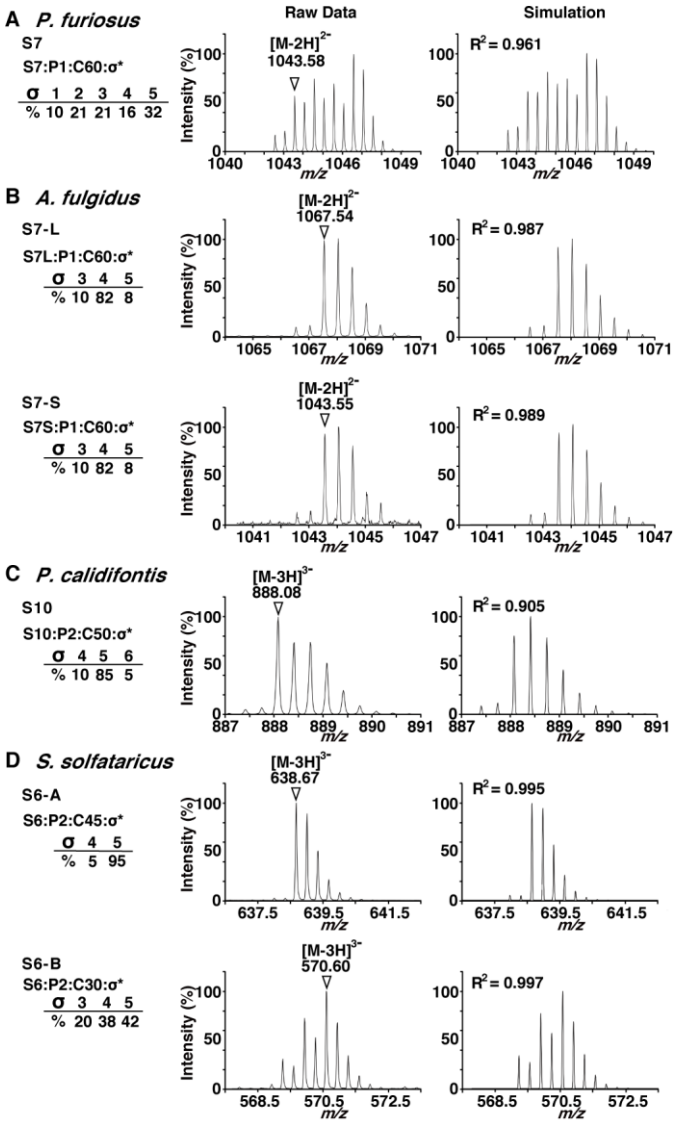

FIGURE 3. **Expansion of the selected TOF-MS ion peaks and comparison with simulated MS spectra.** The most intense ion peaks in the TOF-MS spectra in Fig. 2 were selected, and the expansions of the ion peaks are displayed in the left column. The chemical structure of the ion peaks is represented as S*i*:P*j*:C*k*:□*l*, where *i* is the number of sugar residues, *j* is the number of phosphate groups, *k* is the number of carbon atoms of the dolichol moiety, and *l* is the number of saturated isoprene units. The ions used in the MS/MS analyses (Fig. 4) are indicated by triangles with their *m/z* values. The simulated MS spectra are shown in the right column, to account for the mixed states of the dolichol species with different degrees of isoprene saturation. The R^2 values of the peak intensity correlation between the raw and simulated mass spectra were calculated. Note that the saturation number includes the saturation of the double bond in the □-isoprene unit, which is the signature for the definition of dolichol.

LLO analyzed in this study. Among the LLOs with a C30 dolichol chain, the most saturated species contained only one double bond, among the six isoprene units (Fig. 3D).

MS/MS analyses of the oligosaccharide-charged Dol-P and Dol-PP molecules

The MS/MS analyses were performed to confirm the estimated structures of the LLOs (Fig. 4). To perform the analyses under optimal ESI conditions, the collected fractions were reanalyzed by the direct-infusion ESI method. Ideally, the selected ion for an MS/MS analysis is monoisotopic, to simplify the interpretation by eliminating complicated isotopic

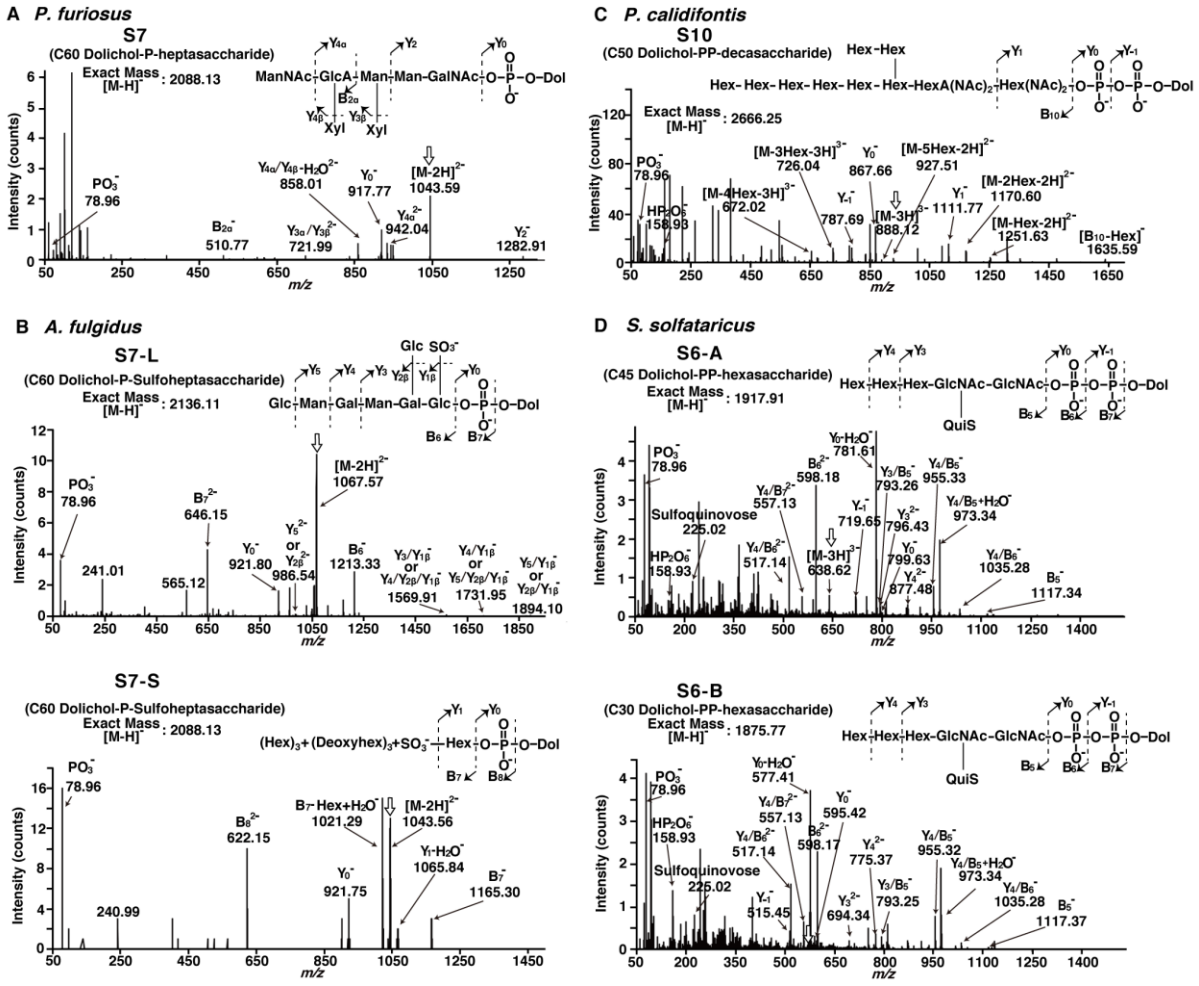

FIGURE 4. **ESI-MS/MS spectra of the oligosaccharide-charged Dol-P and Dol-PP molecules**. The NPLC fractions containing the LLOs were collected and analyzed by direct-infusion ESI-MS/MS in the negative ion mode. The precursor ions are marked by the vertical arrows. The insets show the predicted chemical structures of the oligosaccharide-charged Dol-P and Dol-PP molecules, and their MS/MS fragmentation schemes. The expected *m/z* values were observed within 0.05 of the theoretical mass values.

patterns. In the present analyses, however, due to the various degrees of isoprene saturation, the non-monoisotopic ions originating from LLO species with smaller degrees of isoprene saturation overlapped with the monoisotopic ions. Fortunately, the contributions of the non-monoisotopic ions were negligible, and the interpretation of the MS/MS spectra was straightforward. Under our ESI conditions, bond cleavages mainly occurred within the oligosaccharide portions and phosphate groups. The fragmentation patterns were consistent with the oligosaccharide structures and the number of phosphate groups, as shown in the

insets of Fig. 4. The presence of a pyrophosphate group was evident by the observation of a monovalent $HP_2O_6^-$ ion (*m/z* 158.93).

MS/MS analyses of the dolichol-phospho products after the oligosaccharyl transfer reaction

As mentioned above, no bond cleavages in the dolichol chain were observed under our ESI conditions, which precluded the identification of the lipid part as dolichol. To bypass this difficulty, the enzymatic products, Dol-P or Dol-PP, were generated by the oligosaccharyl transfer reaction. After a prolonged incubation, the reaction solutions were subjected to the NPLC-ESI-MS analysis. The extracted ion chromatograms (XIC, ion chromatogram created by obtaining the summed intensities of the ions in a specified mass range) of the [M-H]- ion of the C60 Dol-P generated by the *A. fulgidus* AglB-L, the $[M-H]^-$ ion of the C50 Dol-P generated by the *P. calidifontis* membrane fractions, and the $[M-H]^-$ ion of the C45 Dol-P

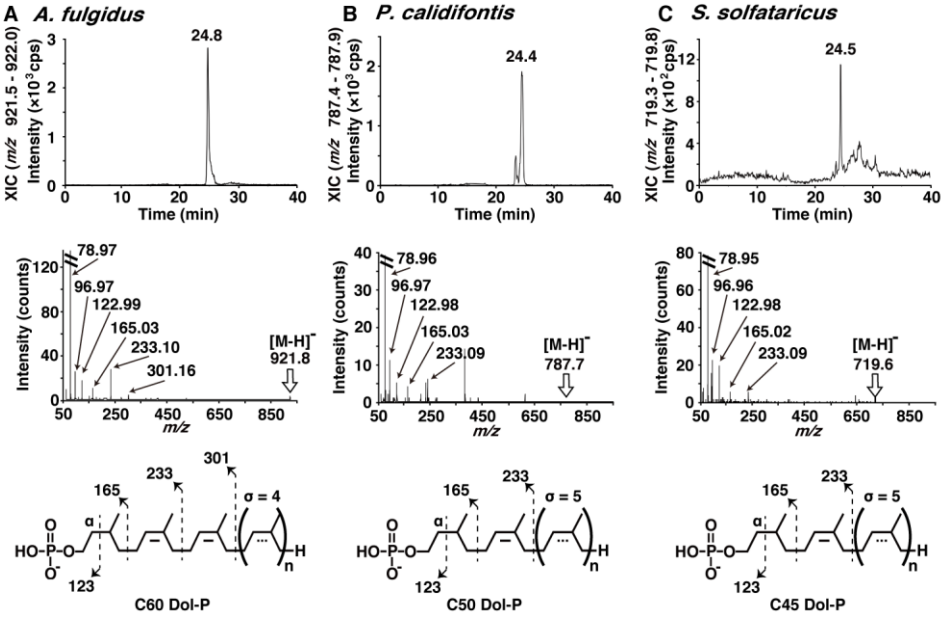

FIGURE 5. **Analysis of the lipid-phosphate products by normal-phase LC and ESI-MS/MS.** The extracted ion chromatograms (XIC) of the NPLC, the ESI-MS/MS spectra, and the fragmentation schemes of the $[M-H]^-$ ions of (*A*) the Dol-P (P1:C60:σ4) generated by the *A. fulgidus* AglB-L, (*B*) the Dol-P (P1:C50:σ5) generated by the *P. calidifontis* LLO-depleted membrane fractions, and (*C*) the Dol-P (P1:C45:σ5) generated by the *S. solfataricus* LLO-depleted membrane fractions. The fragmentation patterns in the MS/MS spectra indicated that the lipid part is dolichol.

generated by the *S. solfataricus* membrane fractions are presented to show the NPLC elution profiles (Fig. 5). The *m/z* values of the generated fragments in the MS/MS spectra were consistent with the presence of theα-saturated isoprene unit in the three archaeal species. Contrary to our expectations, the products derived from the *P. calidifontis* and *S. solfataricus* Dol-PP type LLO was a dolichol-monophosphate molecule. We considered that the generated dolichol-diphosphate was quickly dephosphorylated into the dolichol-monophosphate, by the action of the archaeal counterpart of the DolPP1 phosphatase present in the membrane fractions of *P. calidifontis* and *S. solfataricus*.

For the other LLOs, the α-position saturation was verified as follows. The previous MS analysis indicated that the lipid part of the *P. furiosus* LLO-L was actually dolichol (19). The *A. fulgidus* LLO that is a substrate for *A. fulgidus* AglB-S1 also contains dolichol, because it shares the same lipid-phospho moiety with *A. fulgidus* LLO that is a substrate for *A. fulgidus* AglB-L. This conclusion is justified by considering the similar distributions of the number of isoprene units and the almost identical compositions of the number of isoprene saturations (Figs. 3B and 6B).

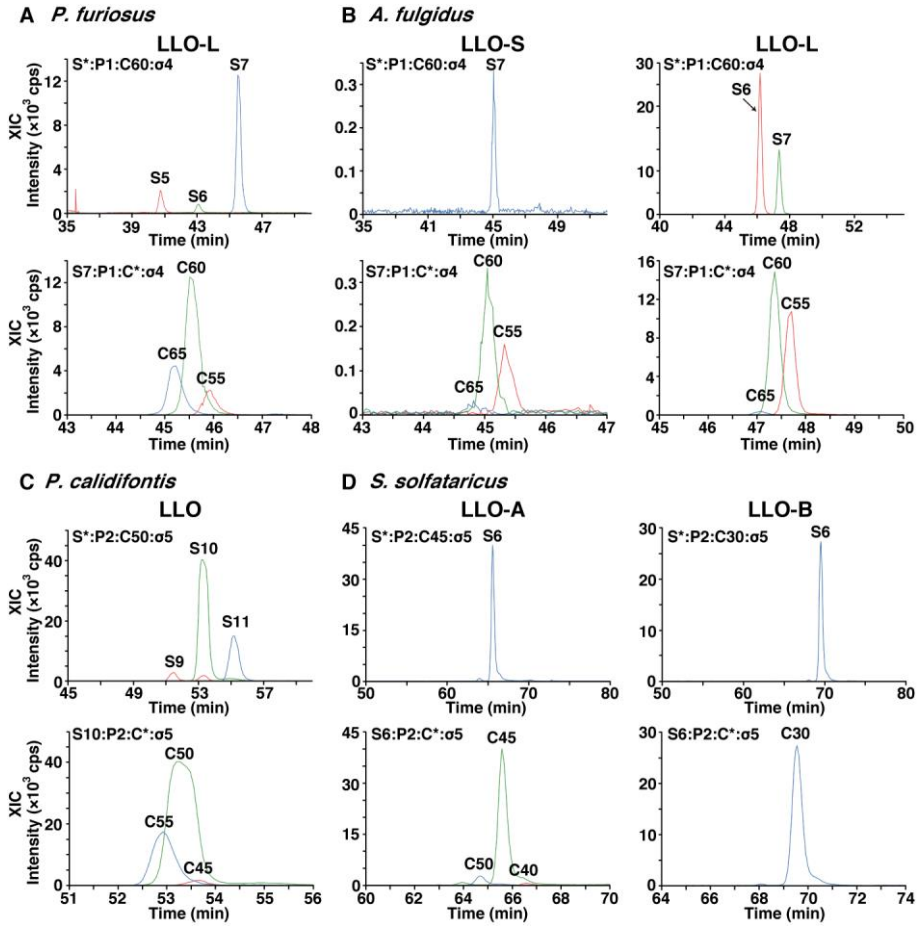

FIGURE 6. **Normal-phase LC XIC profiles for the estimation of the compositions of the LLO species.** The original data are shown in Fig. 2. Ions with different numbers of monosaccharide residues (S5 – S11) or different numbers of carbons in the dolichol moiety (C30 – C65) were selected, to show their extracted ion chromatogram (XIC) profiles. The peak intensities were used to estimate the compositions of the LLO species, in terms of the number of monosaccharide residues and the length of the dolichol chain.

5. DISCUSSION

The domain Archaea is classified into sever alphyla (34). Most of the cultivable and hence well-studied archaeal species are members of two main phyla, the Euryarchaeota and the Crenarchaeota. Other phyla are the Thaumarchaeota, Aigarchaeota, and Korarchaeota. These phyla form the TACK superphylum with Crenarchaeota, and the ancestor of Eukaryotes is suggested to be rooted within the TACK superphylum (35). We selected two species, *P. furiosus* and *A. fulgidus*, from the phylum Euryarchaeota, and two species, *P. calidifontis* and

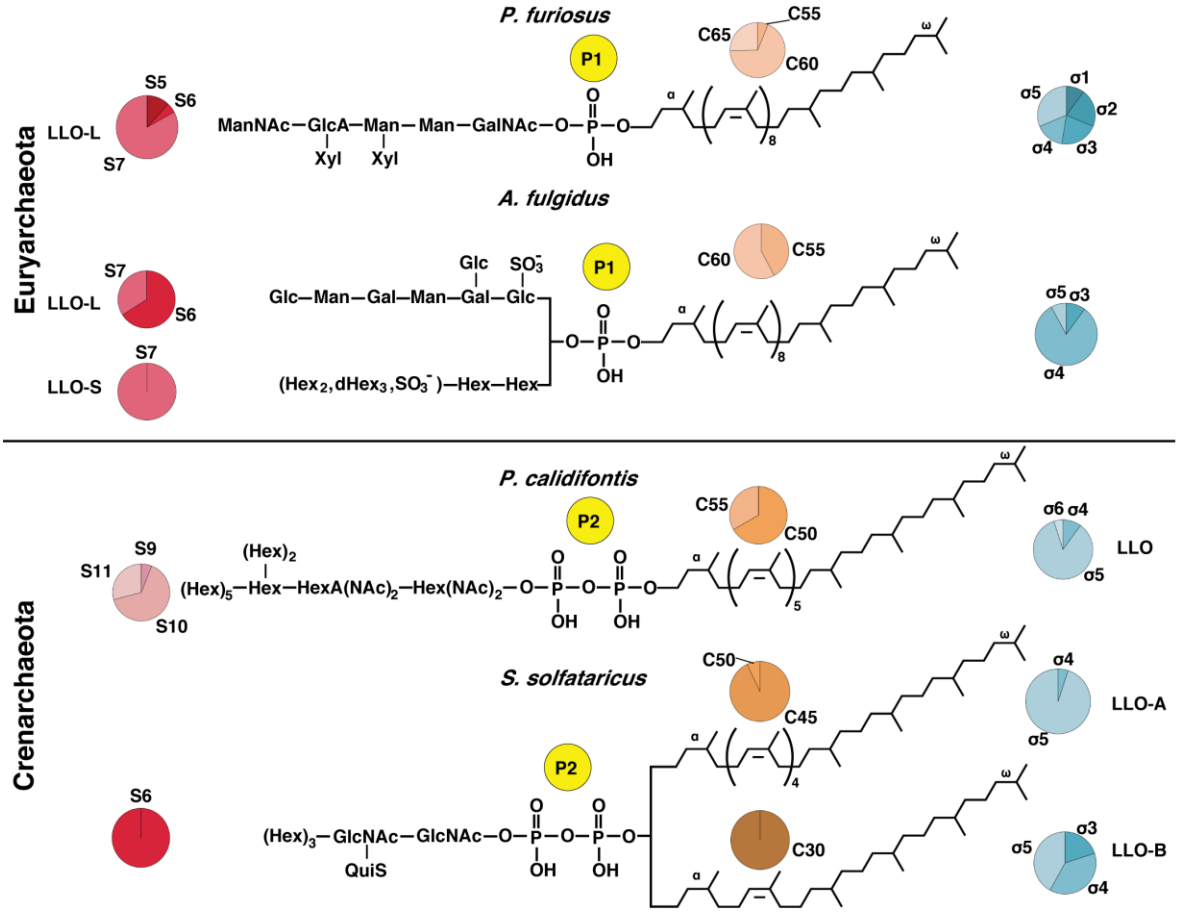

FIGURE 7. **Chemical structures of the archaeal LLOs that serve as oligosaccharide donors for the oligosaccharyl transfer reaction.** The compositions of the number of sugar residues (S), the number of carbon atoms in dolichol (C), and the number of isoprene saturation (σ) are shown in pie charts. Note that the stereochemical features drawn in this figure are not entirely correct. First, the *trans-cis* arrangement of the double bonds in the dolichol chain was assumed to be α-*polycis*-*trans*$_2$-ω for euryarchaeal species, and α-*polycis*-*trans*$_3$-ω for crenarchaeal species (18,46). Secondly, the positions of the saturated isoprene units were assumed to be located from the ω-terminus, except for the α-isoprene unit. Finally, an unidentified atypical stereochemical feature should exist in the dolichol chain of the *S. solfataricus* LLO-B.

S. solfataricus, from the phylum Crenarchaeota, for the comparative study of the structures of LLOs that serve as the donors of the glycans on asparagine residues in proteins. Our aim was comparison to the euryarchaeal LLOs, the crenarchaeal LLOs are less well understood. This is partly due to the unavailability of the recombinant AglB enzymes. To circumvent this issue, we prepared LLO-depleted membrane fractions from the cultured archaeal cells.

The chemical structures of the LLOs from the four archaeal species examined in this study are shown in Fig. 7. The results of the MS/MS analyses of the oligosaccharide moieties are all consistent with the previously determined N-glycan structures. Importantly, we assayed the oligosaccharide donor activity of these LLOs for the oligosaccharyl transfer reaction catalyzed by the AglB enzymes. We estimated the numbers of monosaccharide residues in the oligosaccharide moieties, the numbers of isoprene units, and the degrees of isoprene saturation in the dolichol chains. The XIC charts of the NPLC that were used to elucidate these compositions are summarized in Fig. 6. The present study showed that there are two types of LLOs, with respect tothe number of phosphate groups in the domainArchaea. We concluded that the archaeal species in the Euryarchaeota use Dol-P type LLOs for the N-glycosylation, and those in the Crenarchaeota use the Dol-PP type LLOs for the same purpose. To the best of our knowledge, this is the first experimental verification for the latter fact.

We now discuss the evolutionary aspects of the oligosaccharide transfer reaction onto asparagine resides (Table 1). Considering the number of phosphate groups in the LLOs, the N-oligosaccharide transfer reaction in the phylum Crenarchaeota is evolutionally closer to the eukaryotic system than that in the phylum Euryarchaeota (Fig. 8). This view is justified by the higher homology of the amino-acid sequences of the crenarchaeal AglB enzymes to the eukaryotic STT3 counterparts than to those of the euryarchaeal AglBs (5). The N-glycosylation in the euryarchaeal species is dispensable (36,37), but the disruption of the N-glycosylation system is reportedly lethal in the crenarchaeal species (38), as in Eukaryotes. Thus, the Crenarchaeota provide a more suitable model system that complements the studies of the eukaryotic N-glycosylation system.

The comparison of the oligosaccharide structures found in LLOs and those derived from glycoproteins is particularly interesting. The differences in the oligosaccharide structures suggest that post-transfer modifications of the N-glycans occur. The *S. solfataricus* LLOs

TABLE 1
Comparison of the LLO structures in the three domains of life

Domain	Eubacteria	Archaea						Eukaryota
Phylum	Proteobacteria	Euryarchaeota				Crenarchaeota		Ascomycota
Species [a]	*C. jejuni*	*H. volcanii*	*A. fulgidus*		*P. furiosus*	*M. voltae*	*S. solfataricus*	*P. calidifontis*	*S. cerevisiae*
Number of phosphates	2	1	1		1	1	2	2	2
LLO type		A[b]	L	S	L				
Number of sugars	7	4[c]	7[d]	7	7	3	6[e]	10	14
Linking sugar	$Bac(NAc)_2$[f]	Hex	Glc	Hex	GalNAc	GlcNAc	GlcNAc	$Hex(NAc)_2$	GlcNAc
Lipid carrier	Polyprenol	Dolichol	Dolichol		Dolichol	Dolichol	Dolichol	Dolichol	Dolichol
LLO type							A	B	
Lipid length	C55	C55/60	C55/60		C60	n.d.[g]	C45	C30	C50	C70-C110
Number of saturation	0	2	3-5		1-5	n.d.[g]	5	3-5	4-5	1
Reference	(2,20)	(9,44)	This study		This study, (19)	(22)	This study		This study	(20,26)

[a] *Campylobacter jejuni, Haloferax volcanii, Archaeoglobus fulgidus, Pyrococcus furiosus, Methanococcus voltae, Sulfolobus solfataricus, Pyrobaculum calidifontis,* and *Saccharomyces cerevisiae.*

[b] Three different N-glycan backbone structures were reported in the S-layer protein of *H. volcanii* (45). Here we call them type A, type B, and type C, from the N-terminus. The LLO in this table is the oligosaccharide donor for the type A N-glycan.

[c] The number of monosaccharide residues in the N-glycan on the S-layer glycoprotein is 5, due to the post-transfer addition of a mannose residue.

[d] The number of monosaccharide residues in the LLO-L is 8, as determined in the previous NMR study (24). The glucose supplementation of the culture medium for isotope labeling increased the number of monosaccharide residues.

[e] The number of monosaccharide residues in the N-glycan on glycoproteins is 7 (33), due to the post-transfer addition of a hexose residue.

[f] di-N-acetyl bacillosamine

[g] not determined

contains a hexasaccharide including 3 hexoses (Fig. 7), but the N-glycans from the *S. solfataricus* glycoproteins reportedly included a heptasaccharide containing 4 hexoses (33). Thus, the fourth hexose residue may be transferred to the N-glycans on the glycoproteins. This is the second example of the post-transfer modification of archaeal N-glycans, after the *H. volcanii* N-glycan (9). It is reasonable to assume the existence of LLO that serves as the hexose donor for the post-transfer modification reaction. In fact, we identified a Dol-P-hexose molecule in the crude LLO fractions from *S. solfataricus* (data not shown). In accordance, the presence of a Dol-P-hexose molecule was also reported in the total lipid extract of the closely-related *S. acidocaldarius* cells (18). Thus, the genus *Sulfolobus* has Dol-P-hexose as the monosaccharide donor, in addition to the Dol-PP type LLO as the oligosaccharide donor.

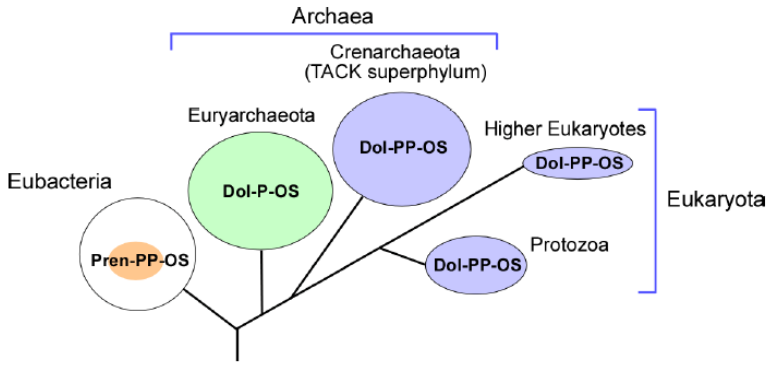

FIGURE 8. **Evolution of LLOs that serve as oligosaccharide donors for the N-oligosaccharyl transfer reaction.** The size of the colored circles is proportional to the structural diversity of the oligosaccharide parts in LLOs. The small colored circle in the large white circle indicates that not all Eubacteria have an N-glycosylation system. Pren, polyprenol; Dol, dolichol; P, monophosphate; PP, diphosphate; OS, oligosaccharide.

Eukaryotic cells also have Dol-P-hexose that serves as the monosaccharide donor for the addition of terminal mannose and glucose residues to complete the synthesis of the 14-residue N-glycan structure on the lumenal face of the ER membranes (8). In Eubacteria, *E. coli* and *Shigella flexneri*, Pren-P-hexose also coexists with the Pren-PP type LLO. Undecaprenol (i.e., C55 polyprenol)-P-glucose is used to modify the O-antigen with a glucose residue for serotype conversion (39). In *E. coli* and *Salmonella enterica*, undecaprenol-P-pentose (4-amino-4-deoxy-L-arabinose) is the monosaccharide donor for the modification of lipid A to increase the resistance to polymyxin antibiotics (40).

One of the most notable aspects of this study is the finding that one archaeal species may contain two distinct LLOs. The first example is the LLOs bearing oligosaccharides with different backbone structures, whereas the number of phosphate groups and the dolichol moieties are common. The present study showed the existence of such LLOs in the *A. fulgidus* cells. The two LLOs were named LLO-L and LLO-S, after AglB-L and AglB-S1, to imply the substrate specificity of the two AglB enzymes. The previous western blot analysis showed that the *A. fulgidus* cells did not express the AglB-S1 or AglB-S2 protein under standard laboratory culture conditions, suggesting that these short AglBs are inducibly controlled (24). However, LLO-S exists in the *A. fulgidus* membranes, even when AglB-S1 and S2 are absent.

The *P. furiosus* genome contains two AglB paralogs, AglB-L and AglB-S. Thus, it is reasonable to assume that the two types of LLOs bearing different oligosaccharide backbone

structures exist in *P. furiosus*. However, we were unable to detect LLO-S in the present NPLC experiments. The failed production of the recombinant AglB-S and the unknown oligosaccharide structure of the putative LLO-S made the MS analysis very difficult. It is possible that LLO-S is not present in the *P. furiosus* membranes under standard laboratory culture conditions. Consistently, the Western blot analysis showed that the *P. furiosus* cells did not express AglB-S (data not shown).

The second example is LLOs bearing dolichols with different backbone structures, while the oligosaccharide parts and the number of phosphate groups are common. In the NPLC chromatogram of the *S. solfataricus* LLO, there were two TIC peaks named S6-A and S6-B (Fig. 2D). Since *S. solfataricus* AglB is encoded by a single gene, the production of glycopeptides by the LLO-depleted membrane fractions (inset of Fig. 2D) suggested that the *S. solfataricus* AglB can use both LLO-A and LLO-B as oligosaccharide donors. The MS/MS analysis revealed that the two LLOs shared the same hexasaccharide containing one sulfoquinovose (QuiS) residue, but the LLO-A contained C45 dolichol and the LLO-B contained C30 dolichol (Figs. 4D and 6D). It is noteworthy that the intermediate-size C35 dolichol species was completely absent in the total lipid extract (Fig. 6D). Intriguingly, the different lengths of the dolichol chains cannot account for the large difference in the elution times in the TIC chart (Fig. 2D). One possible explanation is the difference in the stereochemistry of the dolichol chains, possibly in either the number of trans double bonds in the isoprene units or the absolute configuration of the asymmetric carbon atoms generated by isoprene saturation. The similar retention times of the three Dol-P products in Fig.5 suggests that the basic stereochemistry of the *S. solfataricus* C45 Dol-P (LLO-A) is the same as those of the *A. fulgidus* C60 Dol-P and *P. calidifontis* C50 Dol-P. Thus, the *S. solfataricus* C30 Dol-P (LLO-B) should have an unusual stereochemistry of the dolichol chain. A large-scale preparation and NMR analysis is necessary to elucidate the atypical stereochemical feature.

In summary, some archaeal species contain two distinct LLOs for the N-glycosylation reaction. One type differs in the backbone structure of the oligosaccharide moiety, and another type differs in the backbone structure of the dolichol moiety. Some archaeal genomes encode multiple AglB genes, and possibly as-yet unidentified AglB genes with very low sequence homology, or even functionally homologous enzymes (41). Archaea produce multiple LLOs containing a variety of oligosaccharide and dolichol structures in one organism, and multiple AglB enzymes expressed in either a constitutive or inducible manner

to use these LLOs. This study suggested a second example of the post-transfer modification of the N-glycan in *S. solfataricus.* The complexity of the archaeal N-glycoproteome is probably for the adaptation against harsh environments. The transfer of a tetrasaccharide chain onto the *H. volcanii* S-layer protein in response to low-salt culture conditions provides a good precedent for the adaptation to environmental changes (42). A similar adaptive mechanism was discussed for the lower Eukaryote, Protozoa. The three paralogous STT3 enzymes in *Trypanosoma brucei* have different selectivities for the oligosaccharide moiety in LLO (3,43). The cumulative activity of the three paralogous STT3 enzymes may increase the complexity of the glycoproteome, and eventually facilitate the parasite's survival in mammalian host cells. The present comparative study revealed the wealth of N-glycosylation systems in the domain Archaea (Figs. 7 and 8, and Table 1). Further comparative studies in a wide variety of archaeal species are expected to provide entirely unexpected views of the N-glycosylation systems in the future.

6. ACKNOWLEDGEMENTS

The author wishes to greatly thank Professor Daisuke Kohda (Division of Structural Biology, Graduate school of Systems Life Sciences, Kyushu University, Japan) for their cardinal guidance, helpful advice, valuable discussion, encouragement throughout the study, and opened the way for my future.

The author thanks Dr. Shunsuke Matsumoto (Kyoto Sangyo University, Kyoto, Japan) for the preparation of the recombinant AglB protein and Associate Professor Masaki Matsumoto (Department of Molecular and Cellular Biology, Medical Institue of Bioregulation, Kyushu University) for the advice of the mass spectrometry.

The author grateful to Kohda's laboratory member, Associate Professor Atsushi Shimada, Assistant Professor Kohta Mayanagi, Mr. Daisuke Fujinami, Ms. Miki Otsu, Mr. Takahiro Yamasaki, Ms. Siqin Bala, Ms. Yuki Kawasaki, Ms. Marie Ishikawa, Mr. Shigekazu Koya, Mr. Hajime Motomura and Ms. Xilling Han for their advice and friendship, and to all of the people related in my graduated school life for their kindness and support.

Finally, I 'm great thankful to all my family and friends for their support.

7. REFERENCES

1. Jarrell, K. F., Ding, Y., Meyer, B. H., Albers, S. V., Kaminski, L., and Eichler, J. (2014) N-linked glycosylation in Archaea: a structural, functional, and genetic analysis. *Microbiol. Mol. Biol. Rev.* **78**, 304-341
2. Larkin, A., and Imperiali, B. (2011) The expanding horizons of asparagine-linked glycosylation. *Biochemistry* **50**, 4411-4426
3. Schwarz, F., and Aebi, M. (2011) Mechanisms and principles of N-linked protein glycosylation. *Curr. Opin. Struct. Biol.* **21**, 576-582
4. Aebi, M., Bernasconi, R., Clerc, S., and Molinari, M. (2010) N-glycan structures: recognition and processing in the ER. *Trends Biochem. Sci.* **35**, 74-82
5. Maita, N., Nyirenda, J., Igura, M., Kamishikiryo, J., and Kohda, D. (2010) Comparative structural biology of eubacterial and archaeal oligosaccharyltransferases. *J. Biol. Chem.* **285**, 4941-4950
6. Lizak, C., Gerber, S., Numao, S., Aebi, M., and Locher, K. P. (2011) X-ray structure of a bacterial oligosaccharyltransferase. *Nature* **474**, 350-355
7. Matsumoto, S., Shimada, A., Nyirenda, J., Igura, M., Kawano, Y., and Kohda, D. (2013) Crystal structures of an archaeal oligosaccharyltransferase provide insights into the catalytic cycle of N-linked protein glycosylation. *Proc. Natl. Acad. Sci. U. S. A.* **110**, 17868-17873
8. Lannoo, N., and Van Damme, E. J. (2015) Review/N-glycans: The making of a varied toolbox. *Plant Sci.* **239**, 67-83
9. Guan, Z., Naparstek, S., Kaminski, L., Konrad, Z., and Eichler, J. (2010) Distinct glycan-charged phosphodolichol carriers are required for the assembly of the pentasaccharide N-linked to the Haloferax volcanii S-layer glycoprotein. *Mol. Microbiol.* **78**, 1294-1303
10. Samuelson, J., Banerjee, S., Magnelli, P., Cui, J., Kelleher, D. J., Gilmore, R., and Robbins, P. W. (2005) The diversity of dolichol-linked precursors to Asn-linked glycans likely results from secondary loss of sets of glycosyltransferases. *Proc. Natl. Acad. Sci. U. S. A.* **102**, 1548-1553
11. Magidovich, H., and Eichler, J. (2009) Glycosyltransferases and oligosaccharyltransferases in Archaea: putative components of the N-glycosylation pathway in the third domain of life. *FEMS Microbiol. Lett.* **300**, 122-130
12. Nothaft, H., and Szymanski, C. M. (2013) Bacterial protein N-glycosylation: new perspectives and applications. *J. Biol. Chem.* **288**, 6912-6920

13. Eichler, J. (2013) Extreme sweetness: protein glycosylation in archaea. *Nat Rev Microbiol* **11**, 151-156
14. Meyer, B. H., and Albers, S. V. (2013) Hot and sweet: protein glycosylation in Crenarchaeota. *Biochem. Soc. Trans.* **41**, 384-392
15. Abu-Qarn, M., Yurist-Doutsch, S., Giordano, A., Trauner, A., Morris, H. R., Hitchen, P., Medalia, O., Dell, A., and Eichler, J. (2007) Haloferax volcanii AglB and AglD are involved in N-glycosylation of the S-layer glycoprotein and proper assembly of the surface layer. *J. Mol. Biol.* **374**, 1224-1236
16. Yurist-Doutsch, S., Abu-Qarn, M., Battaglia, F., Morris, H. R., Hitchen, P. G., Dell, A., and Eichler, J. (2008) AglF, aglG and aglI, novel members of a gene island involved in the N-glycosylation of the Haloferax volcanii S-layer glycoprotein. *Mol. Microbiol.* **69**, 1234-1245
17. Cohen-Rosenzweig, C., Guan, Z., Shaanan, B., and Eichler, J. (2014) Substrate promiscuity: AglB, the archaeal oligosaccharyltransferase, can process a variety of lipid-linked glycans. *Appl. Environ. Microbiol.* **80**, 486-496
18. Guan, Z., Meyer, B. H., Albers, S. V., and Eichler, J. (2011) The thermoacidophilic archaeon Sulfolobus acidocaldarius contains an unusually short, highly reduced dolichyl phosphate. *Biochim. Biophys. Acta* **1811**, 607-616
19. Chang, M. M., Imperiali, B., Eichler, J., and Guan, Z. (2015) N-Linked Glycans Are Assembled on Highly Reduced Dolichol Phosphate Carriers in the Hyperthermophilic Archaea Pyrococcus furiosus. *PLoS One* **10**, e0130482
20. Hartley, M. D., and Imperiali, B. (2012) At the membrane frontier: a prospectus on the remarkable evolutionary conservation of polyprenols and polyprenyl-phosphates. *Arch. Biochem. Biophys.* **517**, 83-97
21. Calo, D., Guan, Z., Naparstek, S., and Eichler, J. (2011) Different routes to the same ending: comparing the N-glycosylation processes of Haloferax volcanii and Haloarcula marismortui, two halophilic archaea from the Dead Sea. *Mol. Microbiol.* **81**, 1166-1177
22. Larkin, A., Chang, M. M., Whitworth, G. E., and Imperiali, B. (2013) Biochemical evidence for an alternate pathway in N-linked glycoprotein biosynthesis. *Nat. Chem. Biol.* **9**, 367-373
23. Zeitler, R., Hochmuth, E., Deutzmann, R., and Sumper, M. (1998) Exchange of Ser-4 for Val, Leu or Asn in the sequon Asn-Ala-Ser does not prevent N-glycosylation of the cell surface

glycoprotein from Halobacterium halobium. *Glycobiology* **8**, 1157-1164

24. Fujinami, D., Nyirenda, J., Matsumoto, S., and Kohda, D. (2015) Structural elucidation of an asparagine-linked oligosaccharide from the hyperthermophilic archaeon, Archaeoglobus fulgidus. *Carbohydr. Res.* **413**, 55-62
25. Igura, M., Maita, N., Kamishikiryo, J., Yamada, M., Obita, T., Maenaka, K., and Kohda, D. (2008) Structure-guided identification of a new catalytic motif of oligosaccharyltransferase. *EMBO J.* **27**, 234-243
26. Kelleher, D. J., Karaoglu, D., and Gilmore, R. (2001) Large-scale isolation of dolichol-linked oligosaccharides with homogeneous oligosaccharide structures: determination of steady-state dolichol-linked oligosaccharide compositions. *Glycobiology* **11**, 321-333
27. Gao, N. (2005) Fluorophore-assisted carbohydrate electrophoresis: a sensitive and accurate method for the direct analysis of dolichol pyrophosphate-linked oligosaccharides in cell cultures and tissues. *Methods* **35**, 323-327
28. Igura, M., and Kohda, D. (2011) Selective control of oligosaccharide transfer efficiency for the N-glycosylation sequon by a point mutation in oligosaccharyltransferase. *J. Biol. Chem.* **286**, 13255-13260
29. Matsumoto, S., Igura, M., Nyirenda, J., Matsumoto, M., Yuzawa, S., Noda, N., Inagaki, F., and Kohda, D. (2012) Crystal structure of the C-terminal globular domain of oligosaccharyltransferase from Archaeoglobus fulgidus at 1.75 A resolution. *Biochemistry* **51**, 4157-4166
30. Kohda, D., Yamada, M., Igura, M., Kamishikiryo, J., and Maenaka, K. (2007) New oligosaccharyltransferase assay method. *Glycobiology* **17**, 1175-1182
31. Fujinami, D., Matsumoto, M., Noguchi, T., Sonomoto, K., and Kohda, D. (2014) Structural elucidation of an asparagine-linked oligosaccharide from the hyperthermophilic archaeon, Pyrococcus furiosus. *Carbohydr. Res.* **387**, 30-36
32. Patiny, L., and Borel, A. (2013) ChemCalc: a building block for tomorrow's chemical infrastructure. *J Chem Inf Model* **53**, 1223-1228
33. Palmieri, G., Balestrieri, M., Peter-Katalinic, J., Pohlentz, G., Rossi, M., Fiume, I., and Pocsfalvi, G. (2013) Surface-exposed glycoproteins of hyperthermophilic Sulfolobus solfataricus P2 show a common N-glycosylation profile. *J. Proteome Res.* **12**, 2779-2790

34. Brochier-Armanet, C., Forterre, P., and Gribaldo, S. (2011) Phylogeny and evolution of the Archaea: one hundred genomes later. *Curr. Opin. Microbiol.* **14**, 274-281

35. Koonin, E. V., and Yutin, N. (2014) The dispersed archaeal eukaryome and the complex archaeal ancestor of eukaryotes. *Cold Spring Harb. Perspect. Biol.* **6**, a016188

36. Abu-Qarn, M., and Eichler, J. (2006) Protein N-glycosylation in Archaea: defining Haloferax volcanii genes involved in S-layer glycoprotein glycosylation. *Mol. Microbiol.* **61**, 511-525

37. Chaban, B., Voisin, S., Kelly, J., Logan, S. M., and Jarrell, K. F. (2006) Identification of genes involved in the biosynthesis and attachment of Methanococcus voltae N-linked glycans: insight into N-linked glycosylation pathways in Archaea. *Mol. Microbiol.* **61**, 259-268

38. Meyer, B. H., and Albers, S. V. (2014) AglB, catalyzing the oligosaccharyl transferase step of the archaeal N-glycosylation process, is essential in the thermoacidophilic crenarchaeon Sulfolobus acidocaldarius. *Microbiologyopen* **3**, 531-543

39. Allison, G. E., and Verma, N. K. (2000) Serotype-converting bacteriophages and O-antigen modification in Shigella flexneri. *Trends Microbiol.* **8**, 17-23

40. Trent, M. S., Ribeiro, A. A., Doerrler, W. T., Lin, S., Cotter, R. J., and Raetz, C. R. (2001) Accumulation of a polyisoprene-linked amino sugar in polymyxin-resistant Salmonella typhimurium and Escherichia coli: structural characterization and transfer to lipid A in the periplasm. *J. Biol. Chem.* **276**, 43132-43144

41. Kaminski, L., Guan, Z., Yurist-Doutsch, S., and Eichler, J. (2013) Two distinct N-glycosylation pathways process the Haloferax volcanii S-layer glycoprotein upon changes in environmental salinity. *MBio* **4**, e00716-00713

42. Guan, Z., Naparstek, S., Calo, D., and Eichler, J. (2012) Protein glycosylation as an adaptive response in Archaea: growth at different salt concentrations leads to alterations in Haloferax volcanii S-layer glycoprotein N-glycosylation. *Environ Microbiol* **14**, 743-753

43. Izquierdo, L., Schulz, B. L., Rodrigues, J. A., Guther, M. L., Procter, J. B., Barton, G. J., Aebi, M., and Ferguson, M. A. (2009) Distinct donor and acceptor specificities of Trypanosoma brucei oligosaccharyltransferases. *EMBO J.* **28**, 2650-2661

44. Kuntz, C., Sonnenbichler, J., Sonnenbichler, I., Sumper, M., and Zeitler, R. (1997) Isolation and characterization of dolichol-linked oligosaccharides from Haloferax volcanii. *Glycobiology* **7**, 897-904

45. Parente, J., Casabuono, A., Ferrari, M. C., Paggi, R. A., De Castro, R. E., Couto, A. S., and Gimenez, M. I. (2014) A rhomboid protease gene deletion affects a novel oligosaccharide N-linked to the S-layer glycoprotein of Haloferax volcanii. *J. Biol. Chem.* **289**, 11304-11317

46. Hemmi, H., Yamashita, S., Shimoyama, T., Nakayama, T., and Nishino, T. (2001) Cloning, expression, and characterization of cis-polyprenyl diphosphate synthase from the thermoacidophilic archaeon Sulfolobus acidocaldarius. *J. Bacteriol.* **183**, 401-404